

LOCALIZATION ISSUES IN FORCE-BASED FRAME ELEMENTS

By J Coleman¹ and Enrico Spacone,² Associate Members, ASCE

ABSTRACT: This paper summarizes the results of an investigation on objective modeling and prediction of deformation localization in nonlinear force-based frame elements. Emphasis is placed on the behavior of reinforced concrete structures where localization is most likely to occur. The discussion begins with a brief review of the force-based element formulation. Next, plastic hinge behavior is classified into three categories: hardening plastic hinges, perfectly plastic hinges, and softening plastic hinges. The three types of inelastic behavior pose an increasing challenge to objective postpeak modeling. The physical and numerical characteristics of localized failure are outlined. Two regularization techniques for maintaining postpeak objectivity are proposed: (1) a constant fracture energy criterion, which provides objective response on the element force-displacement level; and (2) geometric scaling, which provides objective response on the local moment-curvature level in plastic hinge regions. The discussion concludes with three applications to different reinforced concrete structures: a frame, a bridge pier, and an overreinforced concrete beam. In all three cases, the proposed regularization technique successfully yields objective model predictions.

INTRODUCTION

Nonlinear frame analysis techniques are finding practical design applications in assessing the performance of building structures and bridges under static and dynamic loads. New performance-based seismic design guidelines (FEMA 1997) require that buildings be analyzed using nonlinear static push-over analyses or nonlinear dynamic analyses to control the global and local demands. The use of nonlinear frame analysis necessitates the availability of robust and computationally efficient models for performing analyses in a reasonable amount of time.

Modeling of material nonlinearities in frame analysis can be classified into two main categories: lumped and distributed plasticity models. The lumped plasticity approach is characterized by inserting discrete nonlinear moment-rotation hinges at the ends of otherwise linear elements. This approach provides an efficient means of modeling and controlling plastic hinge formation. On the other hand, distributed plasticity models provide a more general framework for nonlinear frame analysis, where nonlinearities can develop anywhere along the member. For brittle materials, such as concrete, the behavior of lumped and distributed plasticity models can be compared to that of discrete and smeared crack models in solid finite elements. In the first case, the location and direction of the possible cracks are predetermined, while in the second case, cracks may develop anywhere in the structure. This paper deals with distributed plasticity frame elements.

Two methods are typically followed to formulate distributed plasticity frame models: displacement- and force-based formulations. In the displacement-based formulation, the displacement fields along the element are expressed as functions of the nodal displacements. The assumed displacement fields are approximations of the actual displacement fields; thus several elements per member are used to obtain a good approximation of the exact response. In the force-based formulation, the internal force fields are expressed as functions of the nodal forces. Force-based elements are particularly suited for non-

linear frame analysis because they are exact within the framework of the classical beam theories (Spacone et al. 1996a,b). Because of the precision of force-based elements, only one element per structural member is used, leading to considerable savings in the total number of degrees of freedom in the structural model.

This study focuses on localization issues in force-based elements. It is shown that force-based elements lose objectivity at the local and/or global level, depending on the section constitutive behavior. For elastic-perfectly plastic section responses, the section curvature demands are a function of the number of integration points of the numerical integration scheme used for the element integrals. For strain-softening section responses, both the section curvature demands and the element response (and thus the overall structural response) are sensitive to the number of integration points. Strain localization issues also affect displacement-based frame elements, but the displacement interpolation functions force localization within a single element instead of one integration point. Localization in displacement-based solid finite elements has been thoroughly studied and documented by, among others, Bazant and Oh (1983), Bazant and Planas (1998), and de Borst et al. (1994), and the theory extends to frame elements.

In force-based elements, the strains localize at one integration point only. The force-based element developed by Spacone et al. (1996a,b) is used in this study. The element relies on an accurate and robust state determination technique to find the element forces and stiffness matrix. The fiber section model is used to obtain the section response, and each fiber is assigned a nonlinear uniaxial material law. Emphasis is placed on reinforced concrete (RC) members because of the likelihood of elastic-perfectly plastic or strain-softening type behaviors that promote localization problems. Steel structures, on the other hand, generally exhibit strain-hardening inelastic behavior, for which localization concerns are less pronounced. This study addresses the problem of strain localization in compression only. Tension stiffening in RC structures does not play an important role under service or ultimate loads. Thus the topic of strain localization in tension, although fundamental in solid finite-element analyses, does not significantly affect the response of nonlinear frame analyses under seismic loads.

A thorough analysis of the localization characteristics of force-based elements and a clear, simple solution of the problem is fundamental for the application of nonlinear frame analysis to practical problems. In particular, the following tasks must be accomplished: (1) provide objective prediction of the force-displacement response at the element level; and (2) provide objective prediction of the peak curvature demand at the section level in plastic hinge regions. Accurate results are of

¹California Engineering, 825 Avenue H, Treasure Island, San Francisco, CA 94130; formerly, Grad. Student, Dept. of Civ., Envir., and Arch. Engrg., Univ. of Colorado, Boulder, CO 80309-0428.

²Assoc. Prof., Dept. of Civ., Envir., and Arch. Engrg., Univ. of Colorado, Boulder, CO 80309-0428 (corresponding author).

Note. Associate Editor: Marc Hoit. Discussion open until April 1, 2002. To extend the closing date one month, a written request must be filed with the ASCE Manager of Journals. The manuscript for this paper was submitted for review and possible publication on May 31, 2000; revised May 11, 2001. This paper is part of the *Journal of Structural Engineering*, Vol. 127, No. 11, November, 2001. ©ASCE, ISSN 0733-9445/01/0011-1257-1265/\$8.00 + \$.50 per page. Paper No. 22389.

particular interest in the framework of the performance-based design guidelines (FEMA 1997), which require computation of both global (displacements) and local (interstory drifts, curvatures, and thus strains) response quantities for comparison with predetermined performance limits.

FORCE-BASED FRAME ELEMENT FORMULATION

The force-based frame element formulation by Spacone et al. (1996a,b) is quickly reviewed here. The formulation sheds light on the localization issues discussed in the paper. The element is cast in the framework of the 2D Euler-Bernoulli beam theory with small deformations. The formulation has recently been extended to the Timoshenko beam theory by Martino et al. (2000).

The section forces along the beam are grouped in the section force vector $\mathbf{s}(x) = \{N(x)M(x)\}^T$, where $N(x)$ is the axial load and $M(x)$ is the bending moment. The corresponding section deformation vector $\mathbf{e}(x) = \{\epsilon(x)\phi(x)\}^T$ contains the axial strain $\epsilon(x)$ and the curvature $\phi(x)$. In the force-based formulation, from equilibrium the internal forces $\mathbf{s}(x)$ are written as functions of the nodal forces \mathbf{Q} :

$$\mathbf{s}(x) = \mathbf{N}_\varrho(x)\mathbf{Q} \quad (1)$$

where $\mathbf{N}_\varrho(x)$ are the force interpolation functions that, in the case of the beam, define constant axial force and linear bending moment distributions in equilibrium with the nodal forces \mathbf{Q} . For a nonlinear problem, the section constitutive law is written in the incremental form

$$\Delta \mathbf{e}(x) = \mathbf{f}(x)\Delta \mathbf{s}(x) \quad (2)$$

where $\mathbf{f}(x)$ is the section flexibility matrix. Application of the principle of virtual forces yields the following compatibility equation:

$$\mathbf{F}\Delta \mathbf{Q} = \Delta \mathbf{U} \quad (3)$$

where \mathbf{U} are the nodal displacements and \mathbf{F} is the element flexibility matrix

$$\mathbf{F} = \int_0^L \mathbf{N}_\varrho^T(x)\mathbf{f}(x)\mathbf{N}_\varrho(x) dx \quad (4)$$

The great attraction of the force-based formulation stems from the fact that the interpolation functions $\mathbf{N}_\varrho(x)$ are “exact,” that is, the bending moment is linear and the axial load is constant, irrespective of the material behavior of the beam. As long as the exact force interpolation functions can be determined, the flexibility matrix of (4) is exact. Implementation of the force-based frame element into a general-purpose finite-element program requires a special state determination for the computation of the element forces. Spacone et al. (1996a) provide a consistent method for computing the element forces \mathbf{Q} and the element flexibility matrix \mathbf{F} . The method satisfies equilibrium in a strict sense between section and nodal loads, and compatibility between section deformations and nodal displacements is maintained in an integral sense by satisfying the following equation:

$$\mathbf{U} = \int_0^L \mathbf{N}_\varrho^T(x)\mathbf{e}(x) dx \quad (5)$$

The details of the state determination are omitted here because they do not bring additional information on the localization issues discussed in this paper. It is worth mentioning that the state determination and other variations that have stemmed from the original formulation are numerically very stable, even in complex cases such as RC columns that soften due to the crushing of the concrete in compression.

The element integrals (4) and (5) are evaluated through numerical integration

$$\mathbf{F} \cong \sum_{IP=1}^{NIP} w_{IP} L \mathbf{N}_\varrho^T(x_{IP}) \mathbf{f}(x_{IP}) \mathbf{N}_\varrho(x_{IP}) \quad (6a)$$

$$\mathbf{U} \cong \sum_{IP=1}^{NIP} w_{IP} L \mathbf{N}_\varrho^T(x_{IP}) \mathbf{e}(x_{IP}) \quad (6b)$$

where w_{IP} and x_{IP} indicate the weight and position, respectively, of the integration point IP , and NIP indicates the number of integration points in one element. The product $w_{IP}L$ is the length of the integration point L_{IP} . In the current study, the Gauss-Lobatto integration scheme is used because the first and last integration points always coincide with the end sections, where the maximum bending moment is experienced in a structural member without distributed loads.

In the present work, the fiber section model is used to define the section response. Based on the application of the virtual displacement principle, the section forces $\mathbf{s}(x)$ and the section stiffness matrix $\mathbf{k}(x)$ are computed from the fiber responses. The section flexibility matrix $\mathbf{f}(x)$ is obtained as the inverse of $\mathbf{k}(x)$. Well-established uniaxial cyclic constitutive laws for concrete and steel complete the element formulation. The Kent and Park (1971) law is used for concrete behavior in compression, and concrete is assumed to have no tensile strength. The Menegotto and Pinto (1973) law is used for the reinforcing steel. Finally, the force-based element has been implemented in the general-purpose finite-element analysis program FEAP (Taylor 1999).

LOSS OF OBJECTIVITY AT SECTION AND ELEMENT LEVELS

To illustrate the numerical problems encountered in force-based frame elements when plastic hinges form, we will consider the case of a steel cantilever beam under an imposed transverse tip displacement. A single force-based element is used for the entire member. As the applied tip displacement increases, a plastic hinge forms at the base, where the maximum moment occurs. Fig. 1 illustrates the response of the force-based element for the cantilever beam with an elastic-strain-hardening section behavior. Unloading is prescribed in the final steps to clarify the peak displacement and curvature demands. The base shear is plotted against the tip displacement on the right, and the base curvature (that is, the curvature of the first integration point) is shown on the left. The response is objective at both the element and section levels for models with four or more integration points. Three integration points do not accurately integrate the element integrals; thus the stiffness overprediction in the strain-hardening region.

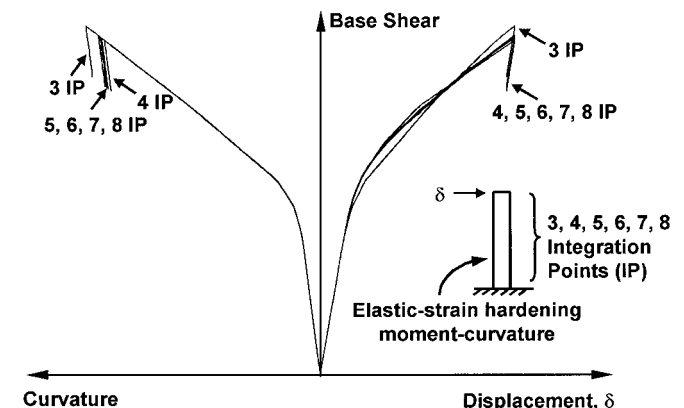


FIG. 1. Cantilever Beam with Elastic-Strain-Hardening Section Response

Fig. 2 shows the response of the same force-based element to an imposed tip displacement with an elastic-perfectly plastic moment-curvature behavior. Here, prediction of the element force-displacement response remains objective while the peak curvature demand varies with the number of integration points. The loss of objective curvature prediction is due to the localization of the inelastic curvature at the base integration point. When this bottom section reaches the plastic moment, the column reaches its load-carrying capacity. As the tip displacement increases, the curvature of the base integration point increases with constant (plastic) moment, while all the other integration points remain linear elastic and do not see any change in either curvature or moment. The length of the base integration point and thus the plastic hinge length becomes a function of the number of integration points used. As the number of integration points increases, the plastic hinge length decreases and the curvature demand in the base integration point must increase to yield the same prescribed tip displacement. From here the nonobjective section prediction of Fig. 2.

In the case of a softening moment-curvature response, the loss of objectivity is more pronounced. Softening section responses may take place in RC columns or in RC bridge piers that support a substantial dead load and are subjected to seismic forces. Fig. 3 illustrates the response of a RC column modeled with a single force-based element. Both the local base section moment-curvature response and the global base shear-displacement response lose objectivity. As the number of integration points increases from three to five, the length of the first integration point decreases and increasing curvatures are required to achieve the same prescribed tip displacement. The concrete fiber compressive strains in the hinge region quickly

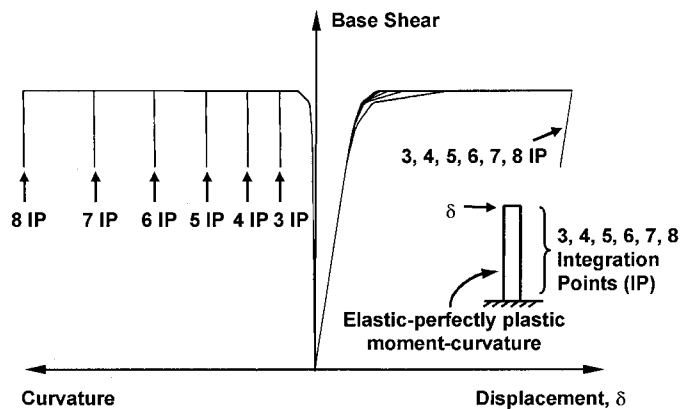


FIG. 2. Cantilever Beam with Elastic-Perfectly Plastic Section Response

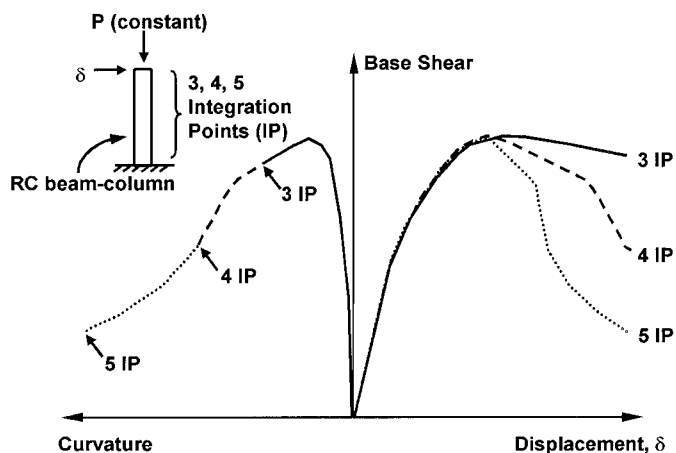


FIG. 3. RC Beam-Column Modeled with Strain-Softening Section Response

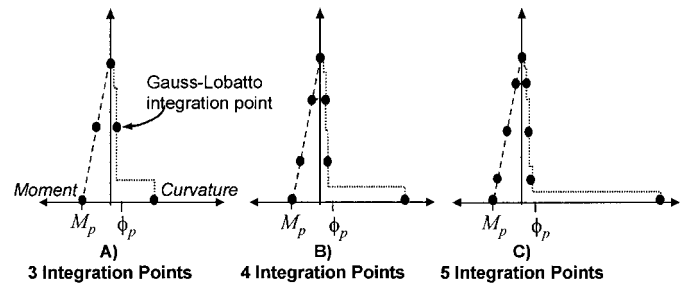


FIG. 4. Moment and Curvature Profiles for Elastic-Perfectly Plastic Cantilever Modeled with Single Force-Based Element

increase, resulting in rapidly degrading material stiffness. For larger numbers of integration points, the postpeak response becomes very brittle and snap-back may occur.

Fig. 4 shows the schematic bending moment and curvature distributions for three, four, and five integration points along the column height. This case refers to the elastic-perfectly plastic section response of Fig. 2 and helps clarify the localization process in force-based elements. The point ϕ_p indicates the plastic curvature when the plastic moment M_p is first reached. Since equilibrium is strictly satisfied in the force-based element, the bending moment remains linear. When the plastic moment M_p is reached at the first (base) integration point, the applied force cannot increase and the tip displacement increases under constant applied load (and constant base moment). Because the bending moment cannot increase beyond M_p , adjacent integration points remain elastic and the inelastic curvature localizes at the first integration point. The tip displacement is computed as the weighted sum of the curvatures at the integration points, as expressed in (6b). The first integration point has a finite length $L_{IP=1} = w_1 L$ proportional to its integration weight w_1 . The larger the number of integration points, the shorter the length of the first integration point and the larger the curvature at the first integration point to obtain the same tip displacement, as shown in Fig. 4.

In summary, it is the ability to capture a jump from elastic to inelastic behavior that makes the force-based formulation both attractive and prone to unique numerical problems. One can observe that as the distance between the first (plastic) and second (elastic) integration point varies, the response also varies. This implies that the number and placement of the integration points not only influences the accuracy of the integration, but also the postpeak response. For hardening materials, plasticity usually spreads beyond a single integration point, and numerical problems are limited to a nonsmooth response if too few integration points are used (Fig. 1). For perfectly plastic and softening cross-section responses, the curvature tends to localize at a particular integration point, and problems with objectivity arise (Figs. 2 and 3).

PHYSICAL CHARACTERISTICS OF LOCALIZED FAILURE IN CONCRETE

In order to introduce the proposed method for reestablishing objectivity of the force-based element response, a brief discussion of the physical characteristics of concrete failure is necessary. Concrete is a heterogeneous material prone to localized failure. In tension, failure is characterized by numerous microcracks that bridge together to form a main crack. The discontinuity induced by the crack opening basically prevents stresses normal to the crack. The failure is termed localized because material outside the fracture process zone remains practically undamaged.

In compression, concrete failure is a different phenomenon. Fig. 5 illustrates a typical laboratory test of a concrete cylinder subjected to uniaxial compression. The test occurs under dis-

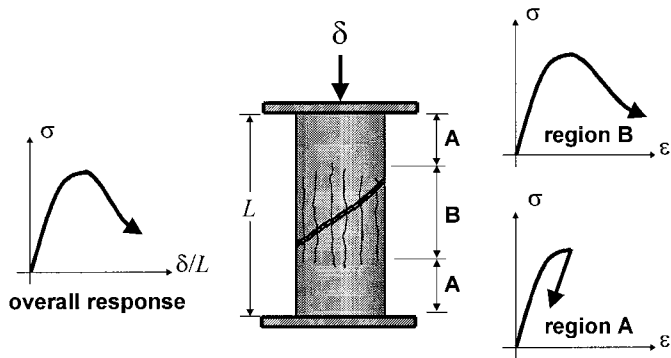


FIG. 5. Uniaxial Compression Test under Displacement Control

placement control in order to capture the postpeak response of the specimen. Region B in Fig. 5 corresponds to a region of damaged concrete. Damage in this region, initially characterized by axial splitting, progresses until a sliding shear band forms and the cylinder stiffness rapidly degrades. The stress-strain curve in this damaged region enters the postpeak branch, where a drop in stress is associated with increasing strains. The concrete in regions labeled A in Fig. 5 is not severely damaged and has not reached the peak strength. To maintain equilibrium of axial force, the stress-strain response in regions A unloads elastically.

The concrete cylinder can be idealized as a series system, where one element (region B in Fig. 5) represents the weak link. When region B reaches the peak strength and starts unloading, the concrete in regions A must unload in order to maintain equilibrium. From these observations it is concluded that concrete failure in compression, as with tension, occurs in a localized manner and requires special attention in a numerical model.

REGULARIZATION TECHNIQUES FOR FORCE-BASED FRAME ELEMENTS

Constant Fracture Energy Criterion

The concept of constant fracture energy in tension is widely used to regularize mesh-sensitive smeared crack displacement-based elements in continuum finite-element analyses by, among others, Bazant and Oh (1983) and Bazant and Planas (1998). The concept is applied here to force-based beam elements that soften in compression. While the constant fracture energy concept is not as widely accepted for compression as it is for tension, recent experimental research (Jansen and Shah 1997; Lee and Willam 1997) and analytical investigations (Markeset and Hillerborg 1995) show that the theory holds true also for localization in compression. The main idea of the regularization process is to assume that the uniaxial stress-strain relation for concrete is supplemented by an additional material parameter, the fracture energy in compression G_f^c , defined as

$$G_f^c = \int \sigma \, du_i \quad (7)$$

where σ is the concrete stress and u_i the inelastic displacement. The integral represents the area under the postpeak portion of the compressive stress-displacement curve. This relation mimics the tensile fracture energy, with a superscript c to indicate compression. To adapt the fracture energy concept to general use, (7) may be cast in terms of stress and strain:

$$G_f^c = h \int \sigma \, d\epsilon_i = L_{IP} \int \sigma \, d\epsilon_i \quad (8)$$

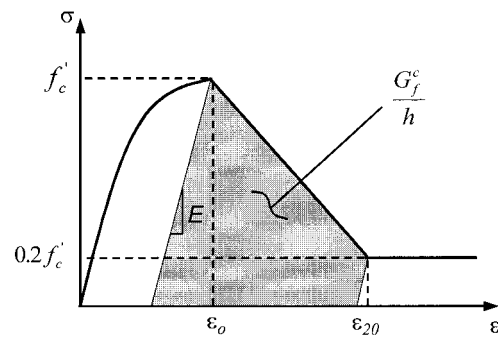


FIG. 6. Kent-Park (1971) Stress-Strain Law and Compression Fracture Energy

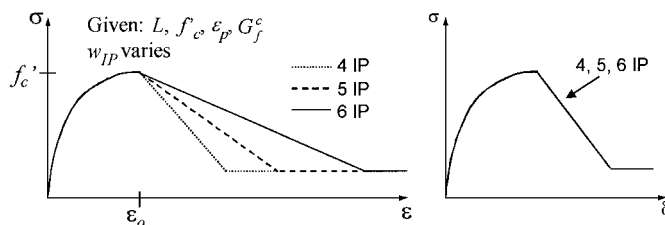


FIG. 7. Stress-Strain Curves with Constant Fracture Energy

where ϵ_i indicates inelastic strain and h is a length scale. For smeared crack elements, h represents the size of a single element in the crack band. For force-based frame elements, h becomes the length of the softening integration point L_{IP} .

Even though the proposed procedure is general, the regularization is applied here to the Kent and Park (1971) law used for the concrete fibers of the fiber section. The prepeak behavior is given by a parabola, followed by a linear postpeak softening branch until a stress of 20% f'_c is reached at a prescribed strain labeled ϵ_{20} . The residual strength is assumed to remain constant for strains larger than ϵ_{20} . The fracture energy is defined here from the peak stress f'_c until the end of the softening branch (Fig. 6). This definition is similar to that of Jansen and Shah (1997), where the fracture energy is defined from the peak stress until 33% f'_c . It follows that ϵ_{20} must be calibrated to maintain a constant energy release. Assuming that G_f^c is known from experimental tests (Jansen and Shah 1997), (8), together with the definition of G_f^c from Fig. 6, leads to the following expression for ϵ_{20} :

$$\epsilon_{20} = \frac{G_f^c}{0.6f'_c L_{IP}} - \frac{0.8f'_c}{E} + \epsilon_0 \quad (9)$$

where E is Young's modulus and ϵ_0 is the strain corresponding to peak stress as indicated in Fig. 6.

Theoretically, (9) implies that the constitutive law must be calibrated for each separate integration point in a structural model. In practice, plastic hinges generally form at the element ends where the extreme integration points lie. If all elements in a model are integrated with the same scheme and number of integration points, ϵ_{20} only varies for elements of element length L . Linking the constitutive law to the element length is a straightforward process.

As the number of integration points increases, the extreme integration point must furnish larger inelastic strains to satisfy the constant fracture energy criteria. This is equivalent to assuming a constant stress-displacement relation rather than a constant stress-strain law, as shown in Fig. 7.

Curvature Postprocessing

Once the global force-displacement response is regularized, in some cases there is still a need to postprocess the results to

obtain an objective prediction of the curvature demand in the plastic hinge region. This is due to the fact that the plastic zone length is the length of the first integration point and does not necessarily correspond to the physical length of the plastic hinge. As with the inelastic strains in a smeared-crack model, the constant fracture energy criterion is insufficient for regularization of the internal element deformations. Because different mesh sizes in a smeared-crack model must produce the same crack opening displacements, the magnitude of inelastic strains must vary. While the inelastic strains in a smeared-crack solid finite element do not have any physical meaning and can remain nonobjective, inelastic curvature demands may be of particular interest in frame elements.

A simple procedure is presented here to obtain an objective prediction of the true curvature demand on the member. Fig. 8 shows a deformed interior beam with plastic hinges forming at both ends. The plastic rotation θ_i and the relevant displacements δ_i are indicated at the near (N) and far (F) ends of the element. These are essentially fictitious quantities used to formulate the curvature scaling law. The bending moment diagram and the curvature profile corresponding to elastic-perfectly plastic behavior are also shown in Fig. 8. Inelastic curvatures, indicated by ϕ_i , are concentrated at the extreme integration points and spread over a length L_{IP} .

The total curvature in the plastic hinge region can be separated into elastic and inelastic curvature components as $\phi = \phi_e + \phi_i$. Considering the geometry of Fig. 8, the inelastic hinge rotation is $\theta_i = \phi_i L_{IP}$. Neglecting the elastic curvature in the other integration points and using a small angle approximation for θ_i , the inelastic curvature can be approximated as

$$\phi_i^{\text{MODEL}} \cong \frac{\delta_i}{L_{IP} \left(\frac{L}{2} - \frac{L_{IP}}{2} \right)} \quad (10)$$

where ϕ_i^{MODEL} indicates the inelastic curvature that results from the analysis. Substituting the actual length of the plastic hinge L_p for L_{IP} yields a similar approximation for the true curvature demand

$$\phi_i^{\text{PREDICT}} \cong \frac{\delta_i}{L_p \left(\frac{L}{2} - \frac{L_p}{2} \right)} \quad (11)$$

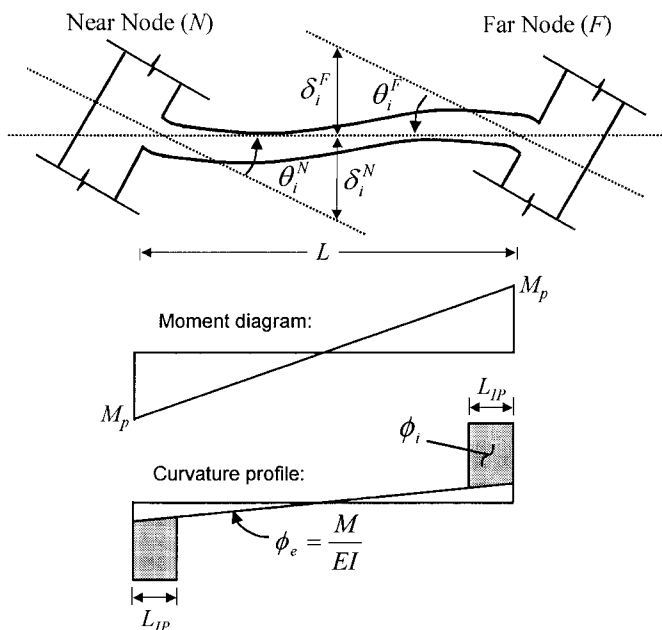


FIG. 8. Interior Beam Forming Plastic Hinges at Both Ends

where ϕ_i^{PREDICT} indicates the inelastic curvature demand based on the assumed plastic hinge length L_p . Finally, the model output can be scaled according to

$$\phi = \phi_e + (\text{scale factor})\phi_i^{\text{MODEL}} \quad (12)$$

where the scale factor is computed by solving for δ_i in (10) and substituting into (11) to obtain

$$\text{scale factor} = \frac{w_{IP} L^2 (1 - w_{IP})}{L_p (L - L_p)} \quad (13)$$

The double-curvature case shown in Fig. 8 prevails in the analyses of buildings under lateral loads. On the other hand, some structural members such as cantilevers experience single curvature, and the plastic hinge forms at one end only. Such is the case of bridge piers subjected to seismic loads in the transverse direction. The double-curvature derivation is readily recast in terms of single curvature by replacing the $L/2$ term in the denominator of (10) and (11) with the full length L . Taking this single-curvature approach results in

$$\text{scale factor} = \frac{w_{IP} L^2 (2 - w_{IP})}{L_p (2L - L_p)} \quad (14)$$

From the previous discussion, it appears that if the length of the first integration point corresponds to the length of the plastic hinge, that is, if $L_{IP} = L_p$, no postprocessing of the curvature is needed because the curvature is objectively predicted by the element. One might then suggest selecting the number of Gauss-Lobatto integration points in such a way that $L_{IP} \cong L_p$. This may cause two problems: (1) the number of integration points may be too small for short elements (causing undesirable reduced integration) or too large for long elements (increasing the computational cost of the element); and (2) in most cases, the length of the element would also have to be adjusted, thus introducing an additional element in each member. This greatly increases the computational cost of the analyses.

Different integration schemes in which the user can define the length of the integration points would also solve the issue, but would significantly compromise the accuracy of the numerical integration. The regularization approach described in this paper is general and does not affect either the element formulation or the integration scheme.

APPLICATIONS

Three applications of the proposed regularization technique will be discussed here. The first is an RC frame with different section behaviors; the second illustrates an RC bridge pier under constant axial load and increasing transverse tip displacement; and the third discusses the test and analytical results of an overreinforced RC simply supported beam.

RC Frame Building

An RC frame is shown in Fig. 9. The beams were designed sufficiently underreinforced and the columns have relatively low axial loads, so that the sections do not show softening responses. The frame is subjected to a monotonically increasing displacement at the top story, with unloading prescribed in the final steps. Unloading clarifies the peak curvature demand in the plastic hinge regions. A single force-based element is used for each structural member.

In the first analysis, the elastic modulus of the steel is $E_0 = 200,000$ MPa, with a strain-hardening ratio of 20%. Fig. 10 summarizes the frame response. The plastic hinge regions are indicated at the final time step and the moment-curvature history is plotted for a typical beam hinge. The global force-displacement response is objective and omitted for brevity.

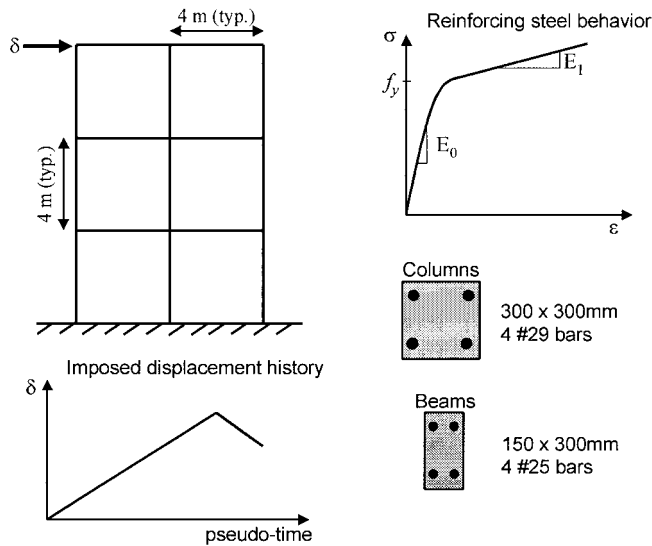


FIG. 9. RC Frame under Applied Displacement

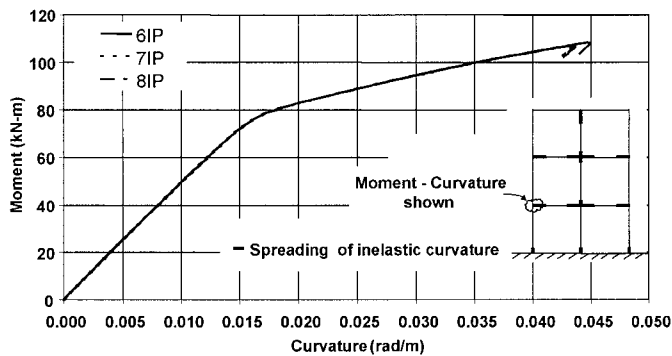


FIG. 10. Response of Six, Seven, and Eight Integration Point (IP) Models with Elastic-Strain Hardening Reinforcing Steel ($E_1 = 0.2 E_0$)

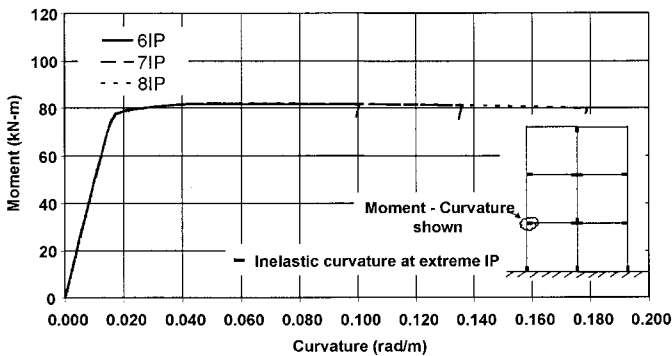


FIG. 11. Response of RC Frame with $E_1 = 0$

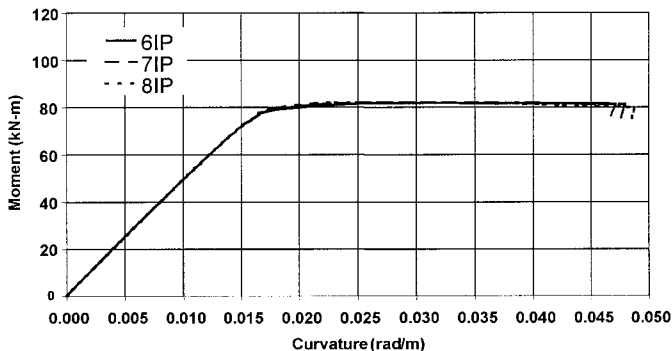


FIG. 12. Regularized Moment-Curvature Response with $E_1 = 0$

The analysis is carried out with six, seven, and eight Gauss-Lobatto integration points. A large number of integration points are used to capture the spreading of inelasticity as strain hardening occurs. As expected, the moment-curvature response is objective: the peak curvature demand remains practically constant as the number of integration points varies.

The frame is then reanalyzed with $E_0 = 200,000$ MPa and zero strain-hardening ratio; that is, the steel is assumed elastic-perfectly plastic. The overall response remains objective for six, seven, and eight integration points, but Fig. 11 shows that the inelastic curvature does not spread but remains localized at the extreme integration points. The moment-curvature history demonstrates a severe loss of objectivity. To regularize the local response, the curvature output for a typical beam hinge is scaled according to (13). Paulay and Priestley's (1992) estimate is used for the plastic hinge length:

$$L_p = 0.08L + 0.022f_y d_b \quad (\text{kN, mm}) \quad (15)$$

The length L in (15) is taken as half the total member length (or 2 m) because the beams are under double curvature; f_y is 420 MPa, and d_b is 25 mm. This gives $L_p = 390$ mm. The weights w_{IP} of the first and last integration points in the Gauss-Lobatto integration scheme are 0.0333, 0.0238, and 0.0179 for six, seven, and eight integration points, respectively. The curvature scale factors are computed as 0.366, 0.264, 0.200 for six, seven, and eight integration points, respectively. Fig. 12 shows the moment-curvature response for the same integration point of Fig. 11 after the regularization is applied.

RC Bridge Pier

Tanaka and Park (1990) describe a series of tests on RC cantilever columns with constant axial load and cyclic tip displacement. The test arrangement approximates the behavior of bridge piers subjected to earthquake ground motion. The geometry of one of these specimens, labeled specimen 7, and the reinforcement arrangement are shown in Fig. 13 and are given by Taylor et al. (1997). The overall monotonic and cyclic experimental response is not of interest in this study, but the column provides an ideal example for showcasing the proposed regularization technique.

A single force-based element is used to model the column. For the reinforcing steel, the initial modulus of elasticity is $E_0 = 200,000$ MPa, with a strain-hardening ratio of 1%. Because of the considerable axial load, the overall column behavior enters the postpeak region and shows strain softening. For concrete, the Kent-Park (1971) law of Fig. 6 is used with $f'_c = 39$ MPa and $\epsilon_0 = 0.0024$ mm/mm. In a first analysis, ϵ_{20} is taken as constant at 0.0248 mm/mm. The analysis is carried out with four, five, and six integration points. This example focuses on the force-displacement response shown in Fig. 14. The first analysis results in force-displacement curves that are extremely

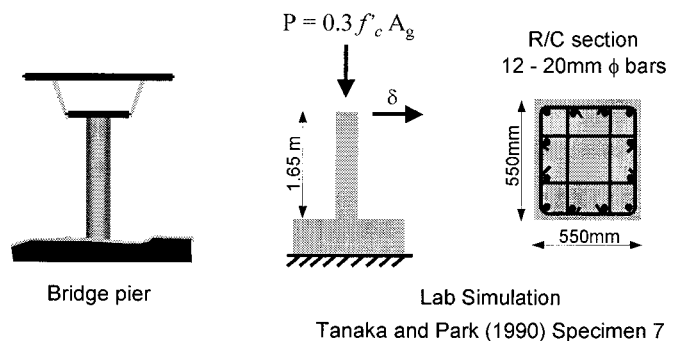


FIG. 13. Softening RC Bridge Pier

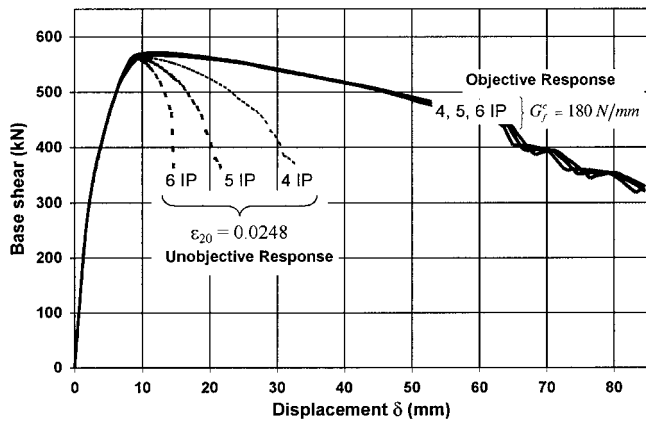


FIG. 14. Force-Displacement Response of Softening Beam-Column

brittle. This is because inelastic curvature localizes in the first integration point, resulting in rapidly increasing strains in the extreme fibers as the test enters the postpeak region.

To regularize the force-displacement response, the compressive fracture energy must be estimated. Cylinder tests of plain concrete usually give fracture energy values of 20 to 30 N/mm. Concrete well confined by steel hoops may have a much higher apparent fracture energy. The compressive fracture energy is here assumed equal to 180 N/mm or about six times that of plain concrete. The constant fracture energy criterion is enforced by adjusting the softening slope of the stress-strain law for concrete according to (9), from which ϵ_{20} is found equal to 0.0573, 0.0946, and 0.1410 mm/mm for the four, five, and six integration point schemes, respectively. Re-running the analysis with the adjusted stress-strain laws gives the regularized response indicated in Fig. 14.

Overreinforced Concrete Beam

The two previous examples encompass practical applications of the proposed regularization techniques. A third example is presented here to explore a popular topic in the research community that concerns an overreinforced beam used for a round-robin numerical test (Ulfkjaer et al. 1997; Ulfkjaer 1998). The test was initiated by the RILEM Technical Committee 148 SSC (Ulfkjaer et al. 1997) to investigate whether current modeling techniques, in combination with standard test data, are sufficient to predict the strain-softening behavior of concrete in compression. The study of this overreinforced beam with a clear postpeak response initially attracted the writers to studying the problem of localization in force-based elements. The beam, shown in Fig. 15, is subjected to a four-point bending test that induces a constant moment in the middle third of the beam. Adequate stirrups are provided to prevent shear failure.

Fig. 16(a) shows a first mesh used to model the overreinforced beam. Because the moment is uniform between the loads, the extreme compression fiber is uniformly compressed in this region. As the beam reaches peak loading, sections (1), (2), and (3) soften uniformly. This is not only inconvenient, since the constant fracture energy criterion is formulated for a single softening integration point, but it is also physically inaccurate. Due to local imperfections and nonuniformities, damage localizes over a limited length. Fig. 16(b) shows a revised model of the overreinforced beam where the middle integration point is assumed to have a slightly lower concrete compressive strength. This triggers strain localization at the weak integration point, which softens while adjacent sections unload to maintain equilibrium.

Assuming a constant value for the softening slope of the

stress-strain curve leads to the nonobjective results shown in Fig. 17. Because the analysis takes place under symmetric displacement control, an odd number of integration points must be used to permit a symmetric failure mode (softening at the middle integration point). The response is regularized by enforcing the constant fracture energy criterion at the weak section. Taking $G_f^c = 20$ N/mm for unconfined concrete (based on the recommendation by Jansen and Shah 1997) results in the force-displacement response shown in Fig. 18 for the model with three integration points at the innermost element. Identical results are obtained with five and seven integration points. The analytical response is superimposed to the experimental data on three identically designed beams. The experi-

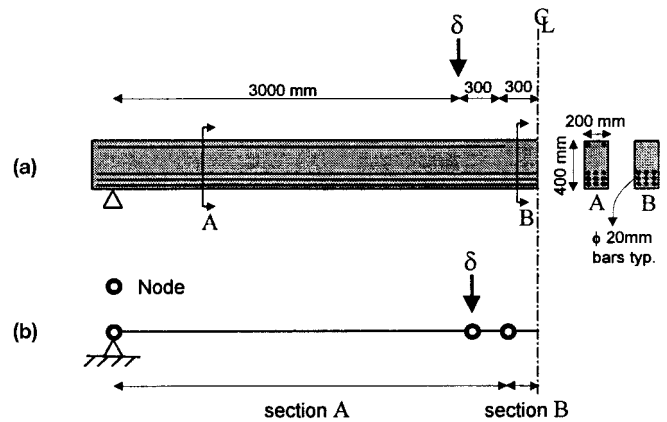


FIG. 15. Overreinforced Beam: (a) Four-Point Bending Test; (b) Numerical Model

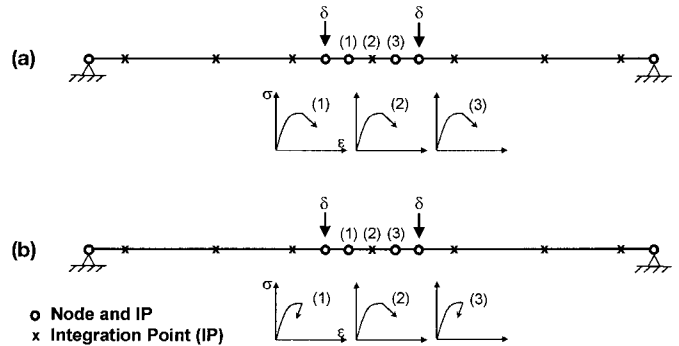


FIG. 16. Numerical Models for Overreinforced Beam: (a) Uniform Softening over One Element; (b) Strain Localization at One Section

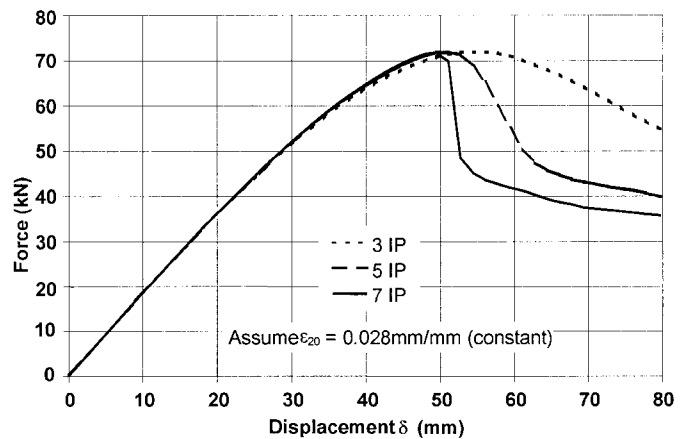


FIG. 17. Nonobjective Response of Overreinforced Beam

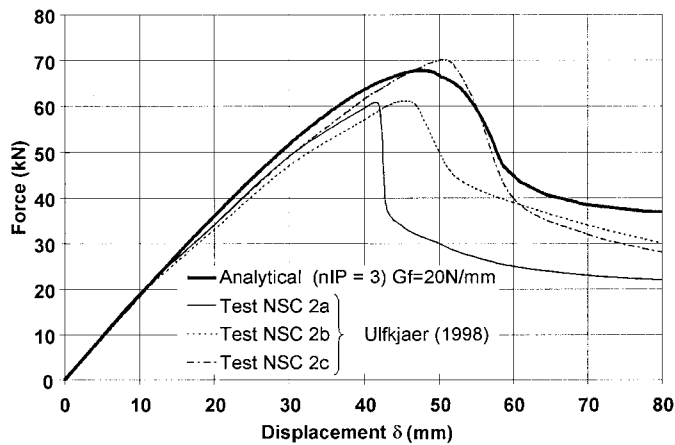


FIG. 18. Overreinforced Beam: Regularized Force-Displacement Response

mental results show the difficulties encountered in running such a brittle test, as well as a wide scatter in both the peak load and postpeak responses.

SUMMARY AND CONCLUSIONS

Force-based frame elements offer an accurate and computationally efficient approach to nonlinear frame analysis because the elements are exact within the framework of the classical beam theories. The main advantage of force-based elements is the ability to model material nonlinearity using a single element per structural member. The numerical integration of the element integrals leads to deformation localization, typically observed at the end integration points where the bending moments reach their maximum. While the above issues are general, this paper deals mostly with RC structures. Three general cases are considered:

- Strain-hardening section response. No localization problems manifest in this case, but a sufficient number of integration points is necessary to guarantee accurate integration and a smooth spreading of inelastic curvature along the member and to avoid abrupt stiffness changes in the response.
- Perfectly plastic response. Sensitivity to the number of integration points is observed in the postyield phase. Deformations localize at the extreme integration points, resulting in a nonobjective curvature prediction that depends on the number of integration points. A simple remedy based on geometric relations is proposed to regularize the curvature demand.
- Strain-softening section response. Loss of objectivity is observed in both the section moment-curvature response and in the element force-displacement response. Enforcing the constant fracture energy criterion in the compression postpeak region regularizes the element response. The proposed stress-strain scaling follows regularization techniques used in smeared crack finite elements. Similar to perfectly plastic sections, geometric regularization of the curvature is also needed after the nonlinear analysis is performed.

The proposed regularization technique for softening sections requires knowledge of the compression fracture energy for the concrete used in the structure, both unconfined and confined. This parameter supplements the concrete stress-strain relation to maintain a constant stress-displacement relation in the postpeak. For the application of the curvature regularization pro-

cedure, the plastic hinge length is computed from empirical equations available in the published literature.

The validity of the proposed regularization technique is shown through three applications, one to an RC frame where plastic hinges form in some members, the second to an RC bridge pier that shows a strain-softening response, and the third to an overreinforced beam characterized by a very brittle postpeak response due to crushing of the concrete in compression. In all three cases, the proposed regularization techniques lead to objective results.

This paper advances the applicability of force-based frame elements by identifying their peculiar strain-localization characteristics, which are different from better-known displacement-based solid finite elements. The numerical robustness of the force-based elements has been shown in a number of publications, even in softening members. Establishing simple but efficient regularization procedures is fundamental for the application of force-based elements to performance-based design of structures, where an objective prediction of the member and section responses is required to compare the predicted structural response to the limit deformations at different performance levels.

ACKNOWLEDGMENTS

This work is partially supported by the National Science Foundation under Grant No. CMS-9804613. This support is gratefully acknowledged. However, opinions expressed in this paper are those of the writers and do not necessarily reflect those of the sponsor. The writers would also like to thank Prof. Giorgio Monti of the University "La Sapienza," Rome, for the constructive discussions on the different regularization techniques.

REFERENCES

- Bazant, Z. P., and Oh, B. H. (1983). "Crack band theory for fracture of concrete." *Mat. and Struct.*, 16, 155–177.
- Bazant, Z. P., and Planas, J. (1998). *Fracture and size effect in concrete and other quasibrittle materials*. CRC Press, Boca Raton, Fla.
- de Borst, R., Feenstra, P. H., Pamin, J., and Sluys, L. J. (1994). "Some current issues in computational mechanics of concrete structures." *Computer modelling of concrete structures, Proc., EURO-C*, H. Mang, N. Bićanić, and R. de Borst, eds., 283–302.
- Federal Emergency Management Agency (FEMA). (1997). "NEHRP guidelines for the seismic rehabilitation of buildings." *Rep. No. FEMA-273*, Washington, D.C.
- Jansen, D. C., and Shah, S. P. (1997). "Effect of length on compressive strain-softening of concrete." *J. Engrg. Mech.*, ASCE, 123(1), 25–35.
- Kent, D. C., and Park, R. (1971). "Flexural members with confined concrete." *J. Struct. Div.*, ASCE, 97(7), 1964–1990.
- Lee, Y.-H., and Willam, K. (1997). "Mechanical properties of concrete in uniaxial compression." *ACI Mat. J.*, 94(6), 457–471.
- Markeset, G., and Hillerborg, A. (1995). "Softening of concrete in compression—Localization and size effects." *Cement and Concrete Res.*, 25(4), 702–708.
- Martino, R., Spacone, E., and Kingsley, G. (2000). "Nonlinear pushover analysis of RC structures." *Advanced technology in structural engineering*, M. Elgahy, ed. (CD-ROM), ASCE, Reston, Va.
- Menegotto, M., and Pinto, P. E. (1973). "Method of analysis for cyclically loaded reinforced concrete plane frames including changes in geometry and nonelastic behavior of elements under combined normal force and bending." *IABSE Symp. on Resistance and Ultimate Deformability of Structures Acted on by Well-Defined Repeated Loads*, IABSE, Zurich, Switzerland, 112–123.
- Paulay, T., and Priestley, M. J. N. (1992). *Seismic design of reinforced concrete and masonry buildings*. Wiley, New York.
- Spacone, E., Filippou, F. C., and Taucer, F. F. (1996a). "Fibre beam-column model for nonlinear analysis of R/C frames. I: Formulation." *Earthquake Engrg. and Struct. Dyn.*, 25(7), 711–725.
- Spacone, E., Filippou, F. C., and Taucer, F. F. (1996b). "Fibre beam-column model for nonlinear analysis of R/C frames. II: Applications." *Earthquake Engrg. and Struct. Dyn.*, 25(7), 727–742.
- Tanaka, H., and Park, R. (1990). "Effect of lateral confining reinforcement on the ductile behaviour of reinforced concrete columns." *Rep. 90-2*, Dept. of Civ. Engrg., University of Canterbury, U.K.
- Taylor, A. W., Kuo, C., Wellenius, K., and Chung, D. (1997). "A sum-

- mary of cyclic lateral load tests on rectangular reinforced concrete columns." *NISTIR 5984*, Bldg. and Fire Res. Lab., National Institute of Standards and Technology, Gaithersburg, Md.
- Taylor, R. L. (1999). *FEAP: A Finite Element Analysis Program; user's manual: Version 7.1*. Dept. of Civ. and Envir. Engrg., University of California, Berkeley, (<http://www.ce.berkeley.edu/~rlt/feap/>).
- Ulfkjaer, J. P. (1998). "Experimental investigation of over-reinforced concrete beams of three different types of concrete and at two different size scales." *Proc., FRAMCOS-3*, AEDIFICATIO Publishers, Gifu, Japan, 1253–1260.
- Ulfkjaer, J. P., van Mier, J. G. M., and Stang, H. (1997). "Invitation to a competition on modeling of over-reinforced concrete beams." *RILEM Tech. Com. 148 SSC Strain Softening of Concrete and ACI/ASCE Committee 447 on Finite Element Anal. of Reinforced Concrete Struct.*